

# Learning Feedback Terms for Reactive Planning and Control

Akshara Rai<sup>2,3,\*</sup>, Giovanni Sutanto<sup>1,2,\*</sup>, Stefan Schaal<sup>1,2</sup> and Franziska Meier<sup>1,2</sup>

**Abstract**—With the advancement of robotics, machine learning, and machine perception, increasingly more robots will enter human environments to assist with daily tasks. However, dynamically-changing human environments requires reactive motion plans. Reactivity can be accomplished through re-planning, e.g. model-predictive control, or through a reactive feedback policy that modifies on-going behavior in response to sensory events. In this paper, we investigate how to use machine learning to add reactivity to a previously learned nominal skilled behavior. We approach this by learning a reactive modification term for movement plans represented by nonlinear differential equations. In particular, we use dynamic movement primitives (DMPs) to represent a skill and a neural network to learn a reactive policy from human demonstrations. We use the well explored domain of obstacle avoidance for robot manipulation as a test bed. Our approach demonstrates how a neural network can be combined with physical insights to ensure robust behavior across different obstacle settings and movement durations. Evaluations on an anthropomorphic robotic system demonstrate the effectiveness of our work.

## I. INTRODUCTION

In order to become effective assistants in natural human environments, robots require a flexible motion planning and control approach. For instance, a simple manipulation task of grasping an object involves a sequence of motions such as moving to the object and grasping it. While executing these plans, several scenarios can create the need to modulate the movement online. Typical examples are reacting to changes in the environment to avoid collisions, or adapting a grasp skill to account for inaccuracies in object representation.

Dynamic movement primitives (DMPs) [1] are one possible motion representation that can potentially be such a reactive feedback controller. DMPs encode kinematic control policies as differential equations with the goal as the attractor. A nonlinear forcing term allows shaping the transient behavior to the attractor without endangering the well-defined attractor properties. Once this nonlinear term has been initialized, e.g., via imitation learning, this movement representation allows for generalization with respect to task parameters such as start, goal, and duration of the movement.

The possibility to add online modulation of a desired behavior is one of the key characteristics of the differential equation formulation of DMPs. This online modulation is achieved via coupling term functions that create a forcing term based on sensory information – thus creating a reactive

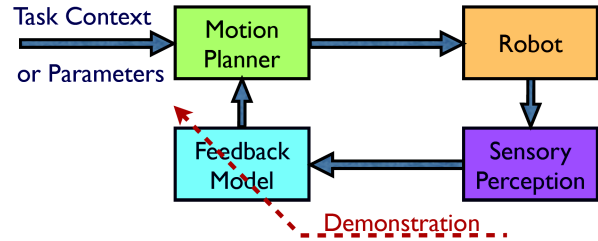


Fig. 1: Proposed framework for learning feedback terms.

controller. The potential of adding feedback terms to the DMP framework has already been shown in a variety of different scenarios, such as modulation for obstacle avoidance [2], [3], [4], [5] and adapting to force and tactile sensor feedback [6], [7]. These approaches have relied on extensive domain knowledge to design the form of the feedback term. But we would like to realize all these behaviors within one unified machine learning framework. This goal opens up several problems such as, how to combine several domain-specific coupling terms without extensive manual intervention and how to design such a compact representation of the coupling term while maintaining generalizability across varying task parameters.

In this paper, we investigate some first steps towards a more general approach to learning coupling term functions. We present contributions along two major axis: Part of our work is concerned with generalizing DMPs with learned forcing and coupling terms. Towards this, we discuss a principled method of creating a local coordinate system of a DMP and creating duration invariant formulations of coupling terms. As a result, demonstrations with different task parameters become comparable. Additionally, we propose to choose a representation of feedback terms that has the inherent potential to incorporate a variety of sensory feedback. Similar to learning the shape of motion primitives - we would like to be able to initialize such a general representation using human demonstrations, to learn the mapping from sensory feedback to coupling term. The overall system diagram is depicted in Figure 1. Given such a general coupling term representation we then would like to incorporate some of the physical intuition – typically used to design the coupling term representation – to create robust and safe behaviors.

This paper is organized as follows. We start out by reviewing background on DMPs and the use of coupling terms in Section II. We then describe how we implement local coordinate transformations within our system in Section III. This is followed by the details of our coupling term learning approach in Section IV. Finally, we evaluate our approach in Section V and conclude with Section VI.

\*both authors contributed equally to this work

<sup>1</sup>CLMC lab, University of Southern California, Los Angeles, USA.

<sup>2</sup>Autonomous Motion Department, MPI-IS, Tübingen, Germany.

<sup>3</sup>Robotics Institute, Carnegie Mellon University, Pittsburgh, USA.

This research was supported in part by National Science Foundation grants IIS-1205249, IIS-1017134, EECS-0926052, the Office of Naval Research, the Okawa Foundation, and the Max-Planck-Society.

## II. BACKGROUND

We need a representation of planning and control for our work that allows for a flexible insertion of machine learning terms to adapt the planned behavior in response to sensory events. Dynamic Movement Primitives (DMPs) [1] are one possibility of such representation, and we adapt the DMP approach for our work due to its convenient and well-established properties.

In brief, DMPs allow us to learn behaviors in terms of nonlinear attractor landscapes. Integrating the DMP equations forward in time creates kinematic trajectory plans, that are converted into motor commands by traditional inverse kinematics and inverse dynamics computations. The DMP differential equations have three components: the main equation that creates the trajectory plan (called a transformation system), a timing system (called canonical system), and a nonlinear function approximation term to shape the attractor landscape (called forcing term). Let  $x$ ,  $\dot{x}$  and  $\ddot{x}$  represent position, velocity and acceleration of the trajectory, then the *transformation system* can be written as follows:

$$\tau^2 \ddot{x} = \alpha_v (\beta_v (g - x) - \tau \dot{x}) + a f + C_t \quad (1)$$

for a one-dimensional system, where  $\tau$  is the movement duration. The nonlinear forcing term  $f$  is scaled by  $a = \frac{g - x_0}{g_{\text{demo}} - x_{0,\text{demo}}}$ , the ratio of distances between the start position  $x_0$  and the goal position  $g$  during unrolling and during demonstration. The *canonical system* defines phase variable  $s$ , representing the current phase of the primitive. This component of the DMP adds the ability to scale a motion primitive to different durations. The canonical system is a first-order dynamical system, given by

$$\tau \dot{s} = -\alpha_s s \quad (2)$$

The transformation system is driven by a nonlinear *forcing term*  $f$  and a coupling term  $C_t$ . The forcing term  $f$  creates the nominal shape of a primitive and is typically modeled as a weighted sum of  $N$  Gaussian basis functions  $\psi_i$  which are functions of the phase  $s$ , with width parameter  $h_i$  and center at  $c_i$ , as follows:

$$f(s) = \frac{\sum_{i=1}^N \psi_i(s) w_i}{\sum_{i=1}^N \psi_i(s)} s \quad (3)$$

where

$$\psi_i(s) = \exp\left(-h_i (s - c_i)^2\right) \quad (4)$$

The forcing term weights  $w_i$  are learned from human demonstration, as pointed out in [1]. The influence of  $f$  vanishes as  $s$  decays to 0, and as a result, position  $x$  converges to the goal at the end of the movement. Beside the forcing term, the transformation system could also be modified by the *coupling term*  $C_t$ , a sensory coupling, which can be either state-dependent or phase-dependent or both.

For a multi degree-of-freedom (DOF) system, each DOF has its own transformation system, but all DOFs share the same canonical system [1].

### A. Coupling Terms

The coupling term  $C_t$  in Equation 1 plays a significant role in this paper and deserves some more discussion. Coupling terms can be used to modify a DMP on-line, based on any state variable of the robot and/or environment. Ideally, a coupling term would be zero unless a special sensory event requires to modify the DMP. One could imagine a coupling term library that handles a variety of situations that require reactive behaviors. In the past, coupling terms have been used to avoid obstacles [5], to avoid joint-limits [8] and to grasp under uncertainty [9]. Coupling terms from previous executions can also be used to associate sensory information with the task, as proposed in [10].

Obstacle avoidance is a classical topic in the motion planning literature. In reference to DMPs, several papers have tried to develop coupling term models that can locally modify the planned DMP to avoid obstacles. Park et al. [2] used a dynamic potential field model to derive a coupling term for obstacle avoidance. Hoffman et al. [3] used a human-inspired model for obstacle avoidance, and Zadeh et al. [4] designed a multiplicative (instead of additive) coupling term. Gams et al. [11] directly modify the forcing term  $f$  of a DMP in an iterative manner and apply it to the task of wiping a surface. This is a step towards automatically learning coupling terms based on experience, rather than hand-designed and hand-tuned models. Chebotar et al. [6] also used reinforcement learning to learn a tactile-sensing coupling term, modulated by tactile feedback from the sensors. More recently, Gams et al. expanded their work in [12], by generating a database of coupling terms and generalizing to multiple scenarios.

All of the above approaches take an iterative approach towards learning the parameters of their coupling term model, but suffer from a lack of generalizability to unseen settings. While any new setting can be learned afresh, there is useful information in every task performed by a robot that can be transferred to other tasks.

Hand-designed features can extract useful information from the environment, but it can be hard to find and tune such hand-designed features. In our previous work [5], we tried to start with human-inspired features for coupling terms from [3] and learn parameters for these features using human demonstrations. This model could generate human-like obstacle avoidance movements for one setting of demonstrations for spherical and cylindrical obstacles. However, it did not generalize across different obstacle avoidance settings. In this paper, we propose a neural-network based coupling model. Given human data this model can be trained to avoid obstacles, and generalizes to multiple obstacle avoidance settings. This eliminates the need for hand-designed features, as well as results in robust obstacle avoidance behavior in unseen settings.

## III. SPATIAL GENERALIZATION USING LOCAL COORDINATE FRAMES

Ijspeert et al. [1] pointed out the importance of a local coordinate system definition for the spatial-generalization of

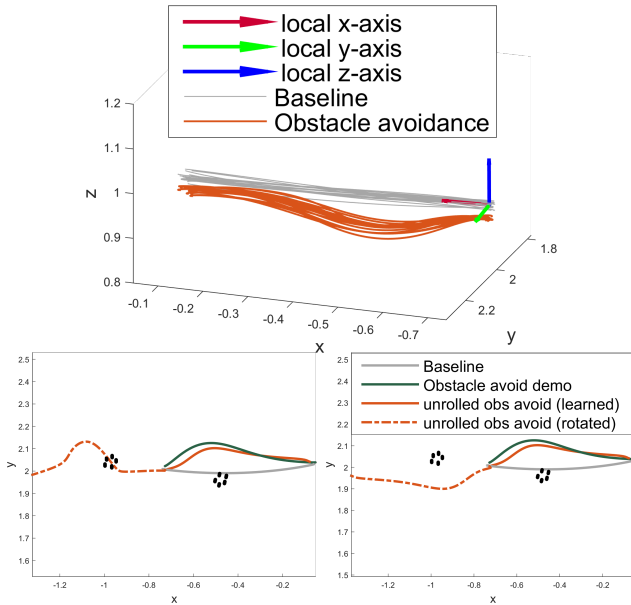


Fig. 2: (top) Example of local coordinate frame definition for a set of obstacle avoidance demonstrations. A local coordinate frame is defined on trajectories collected from human demonstration. (bottom) Unrolled avoidance behavior is shown for two different location of the obstacle and the goal: using local coordinate system definition (bottom right) and not using it (bottom left).

two-dimensional DMPs. Based on this, we define a three-dimensional task space DMPs as follows:

- 1) Local x-axis is the unit vector pointing from the start position towards the goal position.
- 2) Local z-axis is the unit vector orthogonal to the local x-axis and closest to the opposite direction of gravity vector.
- 3) Local y-axis is the unit vector orthogonal to both local x-axis and local z-axis, following the right-hand convention.

The first figure on the top of Figure 2 gives an example of a local coordinate system defined for a set of human obstacle avoidance demonstrations.

The importance of using a local coordinate systems for obstacle avoidance is illustrated in Figure 2 bottom plots. In both plots, black dots represent points on the obstacles. Solid orange trajectories represent the unrolled trajectory of the DMP with learned coupling term when the goal position is the same as the demonstration (dark green). Dotted orange trajectories represent the unrolled trajectory when both goal position and the obstacles are rotated by 180 degrees with respect to the start. DMPs without local coordinate system (bottom left) are unable to generalize the learned coupling term to this new task setting, while DMPs with local coordinate system (bottom right) are able to generalize to the new context. When using local coordinate system, all related variables are transformed into the representation in the local coordinate system before using them as features to compute the coupling term, as described in Figure 3.

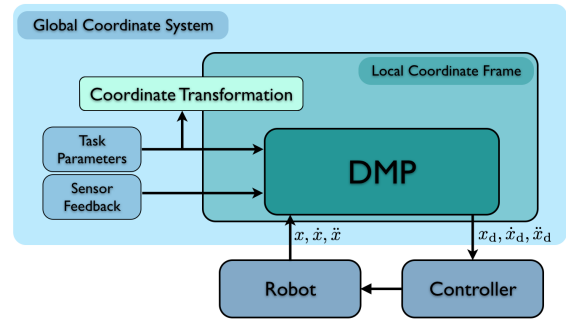


Fig. 3: System overview with local coordinate transform.

#### IV. TOWARDS GENERAL FEEDBACK TERM LEARNING

The larger vision of our work is to create a coupling term learning framework that has the flexibility to incorporate various sensor feedback signals, can be initialized from human data and can generalize to previously unseen scenarios. We envision using coupling terms for objectives other than just obstacle avoidance - for example kinematic and dynamic constraints of a robot, using feedback for tracking, grasping, etc. Towards this goal we present our approach to general feedback term learning in the context of obstacle avoidance. One step towards generalizing to unseen settings is to use a transformed coordinate system, as introduced in Section III. The second challenge of creating a flexible coupling term model is addressed by choosing an appropriate function approximator, that can be fit to predict coupling terms given sensory feedback. Here, we choose to model the coupling term function through a neural network which is trained on human demonstrations of obstacle avoidance. Neural networks have been successfully applied in many different applications – including robotics – and are our function approximator of choice. Typically in robotics, neural networks are used to directly learn the control policy in a model-free way, for example in [13], [14], [15], [16], [17]. In these papers, deep networks directly process the visual input and produce a control output. These approaches use reinforcement learning to learn policies from scratch, or start with locally optimal policies or demonstrations. This results in a very general learning control formulation that, in theory, can generalize to almost any robot or task at hand. In contrast to the common model-free way, we would like to inject structure in our learning through DMPs and use the neural network to locally modulate a global plan created from a trajectory optimizer, or demonstration. We expect such a structure to enable our control to scale to higher dimensions, as well as generalize across different tasks. While there is no question that neural networks have the necessary flexibility to represent a coupling term model with various sensor inputs, there is concern regarding their unconstrained use in real-time control settings. It is likely that the system encounters scenarios that have not been explicitly trained for, for which it is not always clear what a neural network will predict. However, we want to ensure that our network behaves safely in unseen settings. Thus, as

part of our proposed approach, we introduce some physically inspired post processing measures that we apply to our network predictions which ensure safe behaviors including convergence of the motion primitive.

### A. Setting up the learning problem

To learn a general coupling term model from human demonstrations we follow a similar procedure as described in [5]. We start by recording human demonstrations of point-to-point movements, with and without an obstacle on different obstacle settings. The demonstrations without obstacle are used to learn the forcing term function  $\hat{f}(s)$  of the basic dynamic movement primitive representation. All demonstrations with obstacle avoidance behavior are then used to capture the coupling term value with respect to the assumed underlying primitive. For clarity purposes, we refer to the primitive without obstacle avoidance as the baseline to make a distinction from the motion primitive with obstacle avoidance.

The coupling term  $C_t$  of a given demonstration can be computed as the difference of forcing terms between obstacle avoidance behavior and the baseline motion primitive. For a particular obstacle avoidance trajectory, this becomes

$$C_t = \tau^2 \ddot{x}_o - \alpha_v (\beta_v (g - x_o) - \tau \dot{x}_o) - a \hat{f}(s) \quad (5)$$

where  $x_o$ ,  $\dot{x}_o$  and  $\ddot{x}_o$  are the position, velocity and acceleration of the obstacle avoidance trajectory. Since the start and goal positions of the baseline and obstacle avoidance demonstrations are the same in our training demonstrations,  $a = 1$  for the fitting process. Furthermore,  $\tau$  is the movement duration and  $\alpha_v$  and  $\beta_v$  are constants defined in Section II. By computing the difference in forcing terms between the baseline primitive and the obstacle avoidance demonstration, we capture the quantity  $C_t$  that our coupling term model should essentially predict. Further, this formulation makes the target coupling term relatively independent of the baseline trajectory and can also easily handles different lengths of trajectories.

The target coupling term  $C_t$  is calculated for all the demonstrations and concatenated, giving us the regression target  $\mathbf{C}_t$ . Our goal now is to learn a function  $h$ , mapping sensory features  $\mathbf{X}$  – extracted from the demonstrations – to targets  $\mathbf{C}_t$ :

$$\mathbf{C}_t = h(\mathbf{X}) \quad (6)$$

This is a general regression problem which can be addressed using any non-linear function approximator.

### B. Coupling Term Learning with Neural Networks

Neural networks are powerful non-linear function approximators that can be fast and easy to deploy at test time. Given their representational power, neural networks seem to fit into our larger vision of this work. Generally speaking however, any non-linear function approximator could be considered for this part of the framework.

Here, the target coupling term is approximated as the output of our neural network, given sensory features of the obstacle avoidance demonstration.

$$\mathbf{C}_t = h_{\text{NN}}(\mathbf{X}) \quad (7)$$

The inputs  $\mathbf{X}$  are extracted from the obstacle avoidance demonstration. Details of the components of the feature vector  $\mathbf{X}$  are explained in Section V.

Since we consider meaningful input features - that we believe to have an influence on obstacle avoidance behaviors - we do not require the neural network to learn this abstraction, although this would be an interesting avenue for future work. Because of this we only require a shallow neural network, with three small layers only. The hidden layers have rectified linear units (ReLU [18]) and the output layer is a sigmoid, such that the output is bounded. We train one neural network on the three-dimensional target coupling term. Weights and biases are randomly initialized and trained using the Levenberg-Marquardt algorithm. We use the MATLAB Neural Networks toolbox in our experiments [19].

### C. Post-processing the neural network output

Particular care has to be taken when applying neural network predictions in a control loop on a real system. Extrapolation behavior for neural networks can be difficult to predict and comes without any guarantees of reasonable bounds in unseen situations. In a problem like ours, it is nearly impossible to collect data for all possible situations that might be encountered by the robot. As a result, it is important to apply some extra constraints, based on intuition, on the predictions of the neural network. The final coupling term  $C_t$ , given a set of inputs  $x$  becomes

$$C_t = P(h_{\text{NN}}(x)) \quad (8)$$

where  $P$  are the post-processing steps applied to the network's output to ensure safe behavior.

One common problem is that in some situations, we physically expect the coupling term to be 0 or near 0. But due to noise in human data,  $\mathbf{C}_t$  is not necessarily 0 in these cases. For instance, after having avoided the obstacle, we should ensure goal convergence by preventing the coupling term from being active. With such cases in mind, the external constraints applied to the output of the neural network while unrolling are as follows:

- 1) **Set coupling term in x-direction as 0:** In the transformed local coordinate system, the movement of the obstacle avoidance and the baseline trajectory are identical in the x-direction. This means that the coupling term in this dimension can be set to 0. The post-processed coupling term becomes

$$P((C_{tx}, C_{ty}, C_{tz})) = (0, C_{ty}, C_{tz}) \quad (9)$$

- 2) **Exponentially reduce coupling term to 0 on passing the obstacle:** We would like to stop the coupling term once the robot has passed the obstacle, to ensure convergence to the goal. In the local coordinate frame, this

can be easily realized by comparing the x-coordinate of the end effector with the obstacle location. To adjust to the size of the obstacle and multiple obstacles, this post-processing can be modified to take into account obstacle size and the location of the last obstacle. We exponentially reduce the coupling term output in all dimensions once we have passed the obstacle. The post-processing becomes:

$$P(C_t) = \begin{cases} C_t \exp^{-(x_o - x_{ee})^2}, & \text{if } x_o < x_{ee} \\ C_t, & \text{otherwise} \end{cases}$$

where  $x_o$  is the x-coordinate of the obstacle and  $x_{ee}$  is the x-coordinate of the end-effector.

- 3) **Set coupling term to 0 if obstacle is beyond the goal:** If the obstacle is beyond the goal, the coupling term should technically be 0 (as humans do not deviate from the original trajectory). This is easily taken care of by setting the coupling term to 0 in such situations.

$$P(C_t) = \begin{cases} (0, 0, 0), & \text{if } x_o > x_{goal} \\ C_t, & \text{otherwise} \end{cases}$$

where  $x_o$  and  $x_{goal}$  are the x-coordinates of obstacle and goal respectively.

Note, how all the post-processing steps leverage the local coordinate transformation. This post-processing, while not necessarily helping the network generalize to unseen situations, makes it safe for deploying on a real robot. With this learning framework, and the local coordinate transformation we are now ready to tackle the problem of obstacle avoidance using coupling terms. In the next section, we describe our experiments that use this framework to learn a network and then deploy it as a feedback term in the baseline DMP.

## V. EXPERIMENTS

We evaluate our approach in simulation and on a real system. First, we use obstacle avoidance demonstrations collected as detailed below, to extensively evaluate our learning approach in simulation. In the simulated obstacle avoidance setting, we first learn a coupling term model and then unroll the primitive with the learned neural network. We perform three types of experiments: learning/unrolling per single obstacle setting, learning/unrolling across multiple settings and unrolling on unseen settings after learning across multiple settings. We also compare our neural network against the features developed in [5]. This involves defining a grid of hand-designed features and using Bayesian regression with automatic relevance determination to remove the redundant features. We are using three performance metrics to measure the performance of our learning algorithm:

- 1) Training NMSE (normalized mean squared error), calculated as the mean squared error between target and fitted coupling term, normalized by the variance of the regression target:

$$\text{NMSE} = \frac{\frac{1}{N} \sum_{n=1}^N (C_{t,n}^{\text{target}} - C_{t,n}^{\text{fit}})^2}{\text{var}(C_t^{\text{target}})}. \quad (10)$$

where  $N$  is the number of data points.

- 2) Test NMSE on a set of examples held out from the training.
- 3) Closest distance to the obstacle of the obstacle avoidance trajectory.
- 4) Convergence to the goal of the obstacle avoidance trajectory.

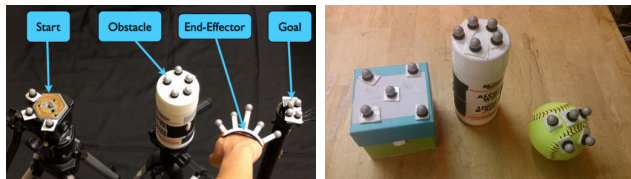
Finally, we train a neural network across multiple settings and deploy it on a real system.

In all our experiments detailed below we use the same neural network structure: The neural network has a depth of 3 layers, with 2 hidden layers with 20 and 10 ReLU units each and an output sigmoid layer. The total number of inputs is 17 and the number of outputs is 3 for the three dimensions of the coupling term.

- 1) vector between 3 points on the obstacle and end-effector (9 inputs)
- 2) vector between obstacle center and end-effector (3 inputs)
- 3) motion duration ( $\tau$ )-multiplied velocity of end-effector ( $\tau\mathbf{v}$ , 3 inputs)
- 4) distance to the obstacle (1 input)
- 5) angle between the end-effector velocity and obstacle (1 input)

### A. Experimental Setup

To record human demonstrations we used a Vicon motion capture system at 25 Hz sampling rate, with markers at the start position, goal position, obstacle positions and the end-effector. These can be seen in Figure 4. In total there are 40

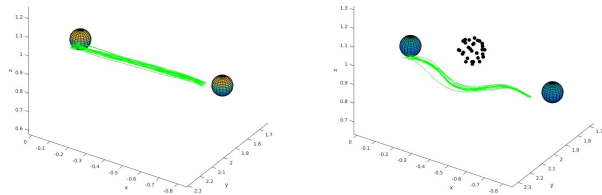


(a) Data collection setting using Vicon objects to represent end-effector, obstacle, start and goal positions. (b) Different types of obstacles used in data collection, from left to right: cube, cylinder, and sphere

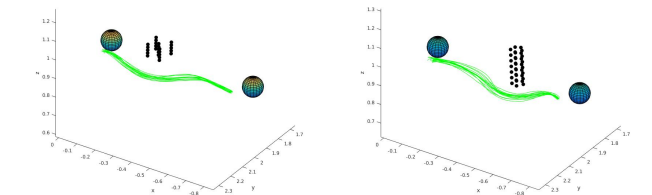
Fig. 4: Data collection setting and different obstacle geometries used in experiment.

different obstacle settings, each corresponding to one obstacle position in the setup. We collected 21 demonstrations for the baseline (no obstacle) behavior and 15 demonstrations of obstacle avoidance for each obstacle settings with three different obstacles – sphere, cube and cylinder. From all baseline demonstrations, we learned one baseline primitive, and all obstacle avoidance behaviors are assumed to be a deviation of the baseline primitive, whose degree of deviation is dependent on the obstacle setting. Some examples of the obstacle avoidance demonstrations can be seen in Figure 5. Even though the Vicon setup only tracked about 4-6 Vicon markers for each obstacle geometry, we augmented

the obstacle representation with more points to represent the volume of each obstacle object.



(a) All nominal/baseline demonstrations (no obstacles). (b) Sphere obstacle avoidance demonstrations.



(c) Cube obstacle avoidance demonstrations. (d) Cylindrical obstacle avoidance demonstrations.

Fig. 5: Sample demonstrations. (b), (c), and (d) are a sample set of demonstrations for 1-out-of-40 settings.

### B. Per setting experiments

The per setting experiments were conducted on each setting separately. We tried to incorporate demonstrations of near and far-away obstacles. In total we test on 120 scenarios, comprised of 40 settings per obstacle type (spheres, cylinder and cube).

A neural network was trained and unrolled over the particular setting in question. For comparison, the model defined in [5] was also trained on the same coupling term target as the neural network. First, we evaluate and compare the ability of the models to fit the training data and generalize to the unseen test data (80/20 split). The consolidated results for these experiments can be found in Figure 6, where we show the training and testing normalized mean square error (NMSE). The top row (plots (a) and (b)) show results over all the scenarios (120) - with the NMSE averaged across the 3 dimensions. The histogram shows, for how many settings we achieved a particular training/testing NMSE. As can be seen, when using the neural network, we achieved an NMSE of 0.1 or lower (for both training and testing data) in all scenarios - indicating that the neural network indeed is flexible enough to fit the data. The same is not true for the model of [5] (plot b). However, a large portion of these settings have the obstacle too far away such that there is no dominant axis of avoidance. The model from [5] has a large training and testing NMSE in such cases. We separated the demonstrations that have a dominant axis of obstacle avoidance (43 scenarios) and show the results for the dominant dimension of obstacle avoidance in plots (c)

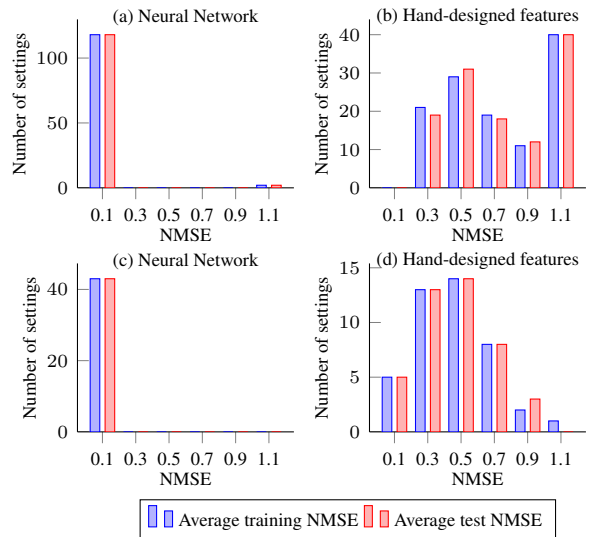


Fig. 6: Histograms describing the results of training and testing using a neural network (left plots) and model from [5] (plots to the right). (a) and (b) are average NMSE across all dimensions generated over the complete dataset. (c) and (d) are the NMSE over the dominant axis of demonstrations with obstacle avoidance.

	Distance to goal		Distance to obstacle		Number of hits
	max	mean	min	mean	
<b>Initial demonstration</b>	0.017	0.017	-0.451	4.992	4
<b>Model from [5]</b>	1.218	0.072	-0.520	5.038	2
<b>Neural Network</b>	0.113	0.016	0.083	5.241	0
<b>Human Demonstration</b>	0.075	0.028	1.409	5.461	0

TABLE I: Results of the per setting experiments. Negative distance to obstacle implies a collision.

and (d) of Figure 6. As expected, the performance of [5] features improves, but is still far behind the performance of the neural network. The features in [5] are unable to fit the human data satisfactorily, as is illustrated in the high training NMSE. On further study, we found that the issue with large regression weights using Bayesian regression with ARD, as mentioned by the authors, can be explained by a mismatch between the coupling term model used and the target set. This also explains why they were not able to fit coupling terms across settings.

The low training NMSE in Figure 6 (a) and (c) show the versatility of our neural network at fitting data very well per setting. Low test errors showed that we were able to fit the data well without over-fitting.

Note that the performance during unrolling for the same obstacle setting can be different from the training demonstrations. When unrolling, the DMP can reach states that were never explored during training, and depending on the generalization of our model, we might end up hitting the obstacle or diverge from our initial trajectory. This brings up two points. One, we want to avoid the obstacle and two, we want to converge to our goal in the prescribed time.

		NMSE		Distance to goal		Distance to obstacle		Number of hits
		train	test	max	mean	mean	min	
Sphere	Baseline	-	-	0.017	0.017	4.739	-0.025	1
	Unrolled	0.155	0.152	0.152	0.018	5.063	0.433	0
Cube	Baseline	-	-	0.017	0.017	5.722	-0.451	1
	Unrolled	0.164	0.159	0.145	0.015	5.964	1.045	0
Cylinder	Baseline	-	-	0.017	0.017	4.514	-0.280	2
	Unrolled	0.195	0.195	0.078	0.014	5.117	0.750	0

TABLE II: Results of the multi setting experiments. Negative distance to obstacle implies a collision.

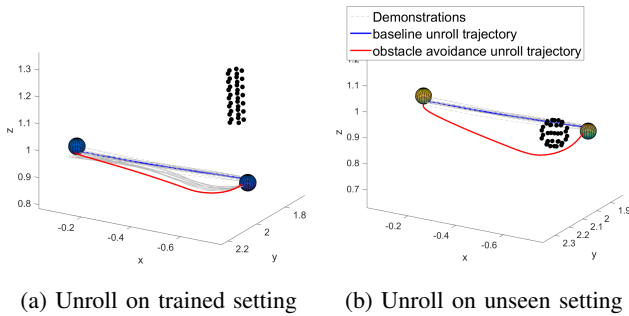


Fig. 7: Sample unrolled trajectories on trained and unseen settings.

We test both methods on these two metrics, and the results are summarized in Table I. We compare the two learned coupling term models to the baseline trajectory, as well as human demonstration of obstacle avoidance. While the neural network never hits the obstacle, the model from [5] hit the obstacle twice. Likewise, the model from [5] does not always converge to the goal, while the neural network always converges to the goal. The mean distance to goal and mean distance from obstacle for both methods are comparable to human demonstrations.

### C. Multiple setting experiments

To test if our model generalizes across multiple settings of obstacle avoidance, we train three neural networks over 40 obstacle avoidance demonstrations per object. The results are summarized in Table II. The neural network has relatively low training and testing NMSE for the three obstacles. To test the unrolling, each of the networks was used to avoid the 40 settings they were trained on. As can be seen from columns 3 and 4, the unrolled trajectories never hit an obstacle. They also converged to the goal in all the unrolled examples. One example of unrolling on a trained setting can be seen in Figure 7a. This shows that our neural network was able to learn coupling terms across multiple settings and produce human-like, reliable obstacle avoidance behavior, unlike previous coupling term models in literature. When we trained our network across all three obstacles, however, the performance deteriorated. We think this is because our chosen inputs are very local in nature and to avoid multiple obstacles the network needs a global input. In the future, we would like to use features that can account for such global information across different obstacles.

### D. Unseen setting experiments

To test generalization across unseen settings, we tested our trained model on 63 unseen settings, initialized on a close  $7 \times 3 \times 3$  grid around the baseline trajectory. We purposely created our unseen settings much harder than the trained settings. Out of 63 settings, the baseline hit the obstacle in 35 demonstrations, as can be seen in Table III. While our models were trained on spheres, cubes and cylinders, they were all tested on spherical obstacles for simplicity. Please note that while a model trained for cylinders can avoid spherical obstacles, behaviorally the unrolled trajectory looks more like that of cylindrical obstacle avoidance, than spherical.

	Distance to goal		Distance to obstacle		Number of hits
	max	mean	mean	min	
Initial	0.017	0.017	0.095	-0.918	35
Sphere	0.011	0.034	0.933	-0.918	2
Cube	0.021	0.119	2.235	1.172	0
Cylinder	0.033	0.120	1.704	-0.103	1

TABLE III: Results of the unseen setting experiments. Negative distance to obstacle implies collision.

As can be seen from Table III, our models were able to generalize to unseen settings quite well. When trained on sphere obstacle settings our approach hit the obstacle in 2 out of 63 settings, when trained on cylinder settings we hit it once, and when trained on cube settings we never hit an obstacle. All the models converged to the goal on all the settings. An example unrolling can be seen in Figure 7b.

### E. Real robot experiment

Finally we deploy the trained neural network on a 7 degree-of-freedom Barrett WAM arm with 300 Hz real-time control rate, and test its performance in avoiding obstacles. We again use Vicon objects tracked in real-time at 25 Hz sampling rate to represent the obstacle. Some snapshots of the robot avoiding a cylindrical obstacle using a neural network trained on multiple cylindrical obstacles can be seen in Figure 8. Video can be seen in <https://youtu.be/hgQzQGcyu0Q>. These are very promising results that show that a neural network with intuitive features and physical constraints can generalize across several settings of obstacle avoidance. It can avoid obstacles in settings never seen before, and converge to the goal in a stable way. This is a starting

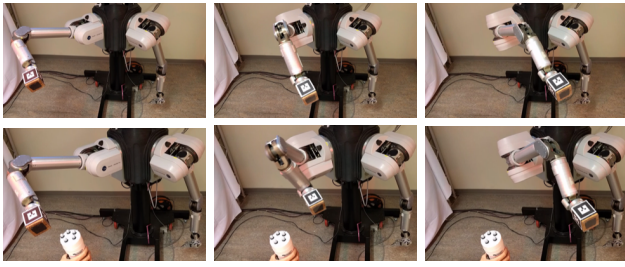


Fig. 8: Snapshots from our experiment on our real system. Here the robot avoids a cylindrical obstacle using a neural network that was trained over cylindrical obstacle avoidance demonstrations. See <https://youtu.be/hgQzQGcyu0Q> for the complete video.

point for learning general feedback terms from data that can generalize robustly to unseen situations.

## VI. DISCUSSION AND FUTURE WORK

In this paper, we introduce a general framework for learning feedback terms from data, and test it on obstacle avoidance. We used a neural network to learn a function that predicts the coupling term given sensory inputs. Our results show that the neural network is able to fit the obstacle avoidance demonstrations per setting as well as over multiple settings. We also proposed to post-process the neural networks' prediction based on physical constraints, that ensured that the obstacle avoidance behavior was always stable and converged to the goal in all the scenarios that we tested. When unrolled on trained settings the DMP with online modulation via the neural network avoided obstacles 100% of the time, and when unrolled on unseen settings 98% of the time. We compared this work to an older coupling term model in [5] and found our new results to be far more impressive, in terms of fitting the data, as well as stability and effectiveness in obstacle avoidance. We also deploy our approach on a 7 degree-of-freedom Barrett WAM arm using a Vicon system and it successfully avoids obstacles.

However, when training across obstacles, the performance of the neural network deteriorates. This could be because generalization across different obstacles needs some global information about the obstacle. In the future, we would like to add some global inputs to try and learn a model across obstacles. Eventually, we would also like to learn coupling terms for tasks other than obstacle avoidance and see the validity of our approach in other problems. Our post-processing too, is focused on obstacle avoidance right now. For more general problems, we might need to add other constraints, for example torque saturation to ensure stable and safe behavior.

The choice of using a neural network was partially influenced by our long term vision of a general approach to learning feedback terms. For instance, it would be interesting to learn a more complex network that takes raw sensor information – such as visual feedback – as input, requiring even lesser human design.

This paper is a step towards automatically learning feedback terms from data and producing safe, generalizable coupling terms that can modify the current plan reactively without re-planning. We are trying to minimize human-designed inputs and tuned parameters in our control approach. Our promising results establish its validity for obstacle avoidance, but how well this performance can be transferred to other tasks still remains to be seen.

## REFERENCES

- [1] A. J. Ijspeert, J. Nakanishi, H. Hoffmann, P. Pastor, and S. Schaal, "Dynamical movement primitives: Learning attractor models for motor behaviors," *Neural Comput.*, vol. 25, no. 2, pp. 328–373, 2013.
- [2] D.-H. Park, H. Hoffmann, P. Pastor, and S. Schaal, "Movement reproduction and obstacle avoidance with dynamic movement primitives and potential fields," in *IEEE International Conference on Humanoid Robots*, 2008, pp. 91–98.
- [3] H. Hoffmann, P. Pastor, D. H. Park, and S. Schaal, "Biologically-inspired dynamical systems for movement generation: Automatic real-time goal adaptation and obstacle avoidance," in *IEEE International Conference on Robotics and Automation*, 2009, pp. 2587–2592.
- [4] S. M. Khansari-Zadeh and A. Billard, "A dynamical system approach to realtime obstacle avoidance," *Auton. Robots*, vol. 32, no. 4, pp. 433–454, 2012.
- [5] A. Rai, F. Meier, A. Ijspeert, and S. Schaal, "Learning coupling terms for obstacle avoidance," in *IEEE-RAS International Conference on Humanoid Robots*, 2014, pp. 512–518.
- [6] Y. Chebotar, O. Kroemer, and J. Peters, "Learning robot tactile sensing for object manipulation," in *IEEE/RSJ International Conference on Intelligent Robots and Systems*, 2014, pp. 3368–3375.
- [7] A. Gams, B. Nemeč, A. J. Ijspeert, and A. Ude, "Coupling movement primitives: Interaction with the environment and bimanual tasks," *IEEE Transactions on Robotics*, vol. 30, no. 4, pp. 816–830, 2014.
- [8] A. Gams, A. J. Ijspeert, S. Schaal, and J. Lenarčič, "On-line learning and modulation of periodic movements with nonlinear dynamical systems," *Autonomous robots*, vol. 27, no. 1, pp. 3–23, 2009.
- [9] P. Pastor, H. Hoffmann, T. Asfour, and S. Schaal, "Learning and generalization of motor skills by learning from demonstration," in *IEEE International Conference on Robotics and Automation*, 2009, pp. 763–768.
- [10] P. Pastor, M. Kalakrishnan, F. Meier, F. Stulp, J. Buchli, E. Theodorou, and S. Schaal, "From dynamic movement primitives to associative skill memories," *Robotics and Autonomous Systems*, vol. 61, no. 4, pp. 351–361, 2013.
- [11] A. Gams, T. Petric, B. Nemeč, and A. Ude, "Learning and adaptation of periodic motion primitives based on force feedback and human coaching interaction," in *IEEE-RAS International Conference on Humanoid Robots*, 2014, pp. 166–171.
- [12] A. Gams, M. Denisa, and A. Ude, "Learning of parametric coupling terms for robot-environment interaction," in *IEEE International Conference on Humanoid Robots*, 2015, pp. 304–309.
- [13] T. P. Lillicrap, J. J. Hunt, A. Pritzel, N. Heess, T. Erez, Y. Tassa, D. Silver, and D. Wierstra, "Continuous control with deep reinforcement learning," *arXiv preprint arXiv:1509.02971*, 2015.
- [14] S. Levine, C. Finn, T. Darrell, and P. Abbeel, "End-to-end training of deep visuomotor policies," *Journal of Machine Learning Research*, vol. 17, no. 39, pp. 1–40, 2016.
- [15] L. Pinto and A. Gupta, "Supersizing self-supervision: Learning to grasp from 50k tries and 700 robot hours," in *IEEE International Conference on Robotics and Automation*, 2016, pp. 3406–3413.
- [16] F. Zhang, J. Leitner, M. Milford, B. Upcroft, and P. Corke, "Towards vision-based deep reinforcement learning for robotic motion control," *arXiv preprint arXiv:1511.03791*, 2015.
- [17] S. Gu, E. Holly, T. Lillicrap, and S. Levine, "Deep reinforcement learning for robotic manipulation with asynchronous off-policy updates," *arXiv preprint arXiv:1610.00633*, 2016.
- [18] V. Nair and G. E. Hinton, "Rectified linear units improve restricted boltzmann machines," in *International Conference on Machine Learning*, 2010, pp. 807–814.
- [19] MATLAB, *MATLAB and Neural Network Toolbox Release 2015a*. Natick, Massachusetts: The MathWorks Inc., 2015.